The growth of an ordered Mn layer on the Si(111)- 1 × 1–Ho surface

2009 J. Phys.: Condens. Matter 21 265001

(http://iopscience.iop.org/0953-8984/21/26/265001)

J. Phys.: Condens. Matter **21** (2009) 265001 (7pp) doi:10.1088/0953-8984/21/26/265001

The growth of an ordered Mn layer on the Si(111)-1 × 1–Ho surface

Michael B Reakes, Chris Eames and Steve P Tear

Department of Physics, University of York, Heslington, York YO10 5DD, UK

Received 23 February 2009, in final form 22 April 2009
Published 27 May 2009
Online at stacks.iop.org/JPhysCM/21/265001

Abstract

The growth of ordered Mn layers on room temperature and liquid nitrogen cooled Si(111)-1 × 1–Ho surfaces has been studied using scanning tunnelling microscopy. We have shown for 4 ML (monolayers) of Mn grown on a cooled Si(111)-1 × 1–Ho surface that an ordered Mn layer is produced without any, or with only limited, silicide formation. This surface exhibits a $(\sqrt{3} \times \sqrt{3})$R30° low energy electron diffraction pattern. Significant variations in Mn island sizes have also been seen on the Si(111)-1 × 1–Ho and Si(111)-7 × 7 surfaces for Mn deposited at room temperature and at −180 °C.

(Some figures in this article are in colour only in the electronic version)

1. Introduction

In recent years the growth of magnetic thin films on semiconductor materials has received increased attention due to their potential use in the growing field of spintronics. Much of the focus has been on Fe silicide thin films with the silicides of antiferromagnetic Mn receiving less attention. However, although Mn is antiferromagnetic in its bulk state it has been predicted to have a large magnetic moment in low dimensional structures such as thin films or nanoclusters [1, 2]. This large magnetic moment makes Mn and Mn silicides potential materials for use in spintronics devices [3]. Mn silicides are also used in the development of optoelectronic devices and thermoelectric materials [4, 5].

Much of the work on Mn systems has dealt with Mn nanoclusters and Mn silicide formation on the Si(111) surface [3, 6–12]. For low Mn coverages (<0.5 monolayer (ML)) deposited at room temperature (RT), Mn clusters have been seen to form well-ordered arrays in the potential wells of the faulted half of the unit cells of the Si(111)-7 × 7 surface [8, 10]. When annealed to around 350 °C these nanoclusters can form near-complete layers of Mn silicide [7]. For coverages of <1 ML annealed at 250 °C a 1 × 1 low energy electron diffraction (LEED) pattern is produced while a $(\sqrt{3} \times \sqrt{3})$R30° LEED pattern is produced for coverages of 4–5 ML annealed at 350 °C [3, 7].

The growth of thin Mn metal layers on the Au(111), Al(111) and Cu(111) surfaces has also been studied [13–15]. For low coverages (<4 ML) a 1 × 1 LEED pattern was observed, with a $(\sqrt{3} \times \sqrt{3})$R30° LEED pattern seen for higher coverages (>4–6 ML). For the higher coverage on Al(111), a morphology transition from fcc Mn into the cubic crystal structure of Mn is suggested coinciding with the change in LEED pattern [13].

The rare earth (RE) silicides have shown potential for technological applications due to good epitaxial growth on the Si(111) surface [16–18]. For 1 ML of RE deposited at 500 °C a Si(111)-1 × 1–Ho surface, or 2D Ho silicide, is formed consisting of a single ML of RE atoms positioned above T4 sites of the bulk-terminated Si(111) surface. Above the RE layer sits a buckled bilayer of Si which is reverse buckled with respect to the Si bulk [19, 20]. The presence of the subsurface RE atoms passivates the surface Si leading to a layer structurally similar to bulk-terminated Si. Good epitaxial growth combined with a passive Si surface make the RE silicides an ideal candidate to form a buffer layer between the clean Si(111) surface and a Mn layer. The Si(111)-1 × 1–Ho surface has been used for further growth in previous studies but not as a buffer layer [21, 22]. A previous study which used Au as a buffer layer to prevent Fe silicide formation on a cooled Si(100) surface met with limited success [23]. Although only limited silicide formation at lower temperatures was achieved, full silicide formation was triggered once the temperature returned to RT.

In this work, the 2D Ho silicide layer is used as a buffer layer to reduce the diffusion of Mn into the Si bulk and to prevent any reaction between the deposited Mn and the surface Si. Importantly, we have cooled samples with liquid nitrogen during Mn deposition to reduce the mobility of the deposited Mn atoms on the Si(111)-1 × 1–Ho surface. This cooling

phase is shown to prevent large Mn island formation and also contributes towards the prevention of initial reactions between the Si bilayer and the deposited Mn. A short 1 min anneal is used to demonstrate the effects of the temperature change during the initial growth of Mn. Samples described as RT refer to a room temperature deposit of Mn and cooled samples refer to samples where Mn was deposited at −180 °C. The results of Mn growth on the 2D Ho silicide and the Si(111)-7 × 7 surfaces are compared under similar growth conditions.

2. Experimental details

Scanning tunnelling microscopy (STM) experiments were performed in a RT Omicron Nanotechnology GmbH STM system with a typical base pressure of 2×10^{-10} mbar. Si(111) samples were cut from a lightly doped n-type wafer and were outgassed for 15 h at 650 °C. Temperature measurements were taken using an infrared pyrometer. The Si surface was prepared by direct current heating at 1200 °C for 1 min followed by a slow cool from 900 to 700 °C. LEED was used to confirm the presence of a well-ordered 7 × 7 reconstruction before 1 ML of Ho was deposited under reactive deposition epitaxy (RDE) conditions at 500 °C (where a ML coverage is defined as 7.88×10^{18} atoms m^{-2} for the Si(111)-1 × 1 surface). A further 10 min anneal at 500 °C and a 5 min anneal at 300 °C were performed to allow a well-ordered Si(111)-1 × 1–Ho surface to form. Although 500 °C is considered to be the optimal silicide formation temperature, the lower temperature of 300 °C reduces the lattice mismatch between the silicon surface and the Si(111)-1 × 1–Ho layer producing higher quality epitaxial growth [24]. Ho was deposited from an evaporation source of our own design consisting of Ho metal in a tantalum boat. This source was calibrated using a quartz crystal microbalance. The formation and quality of the Si(111)-1 × 1–Ho surface was checked by LEED and scanning tunnelling microscopy (STM). LEED was used to confirm a sharp 1 × 1 pattern and STM for the presence of large (40 nm × 40 nm) defect free regions of Si(111)-1 × 1–Ho. Mn was deposited from a Knudsen cell for a short (5–10 min) period on to either RT or cooled 2D Ho silicide. For cooled samples, once the Si(111)-1 × 1–Ho surface was formed, liquid nitrogen was used to cool to a temperature of −180 °C. The short deposit time was used to prevent excess heating of the cooled sample and manipulator by the Knudsen cell. Once the Mn was deposited some samples were annealed at 300 °C for 1 min and allowed to cool to RT before scanning in the STM. Samples which were not annealed were scanned whilst still cool. For the RT Mn silicide sample, the clean Si(111)-7 × 7 surface was allowed to cool to RT after the flash clean followed by a short deposit (5–10 min) of Mn followed by an anneal at either 300 °C for 1 min or 350 °C for 15 min. For the cooled Mn on Si samples, the Si(111)-7 × 7 surface was cooled to −180 °C using liquid nitrogen before Mn deposition. Samples were scanned with STM directly following cooling to ensure they were imaged prior to any annealing effects which might result from the return to RT. Cooling was not available during scanning, but images can be considered to have been taken with the sample above the −180 °C deposit temperature but below RT.

3. Results and discussion

Firstly, we will compare the growth of Mn on the RT Si(111)-7 × 7 and Si(111)-1 × 1–Ho surfaces to demonstrate the effectiveness of the 2D Ho silicide as a buffer layer. Secondly, the influence of cooling during Mn deposition on the Si(111)-1 × 1–Ho and Si(111)-7 × 7 surfaces and the subsequent formation of an ordered Mn layer following an anneal on the Si(111)-1 × 1–Ho surface will be presented.

3.1. The Si(111)-1 × 1–Ho surface as an effective buffer layer for RT growth

A comparison of figures 1(a)–(c) illustrates the effectiveness of the RT Si(111)-1 × 1–Ho surface as a buffer layer. Figure 1(a) shows a clean Si(111)-1 × 1–Ho surface. A step edge can be seen through the centre of the image and incomplete regions of the 2D Ho silicide can be seen as dark regions. Islands of 3D Ho silicide appear bright in the image and are due to a slight over deposit during sample preparation. Some double-tip effects can be seen on these islands.

Mn deposited onto this surface at RT and annealed at 300 °C for 1 min results in a weak (1 × 1) LEED pattern and STM images (figure 1(b)) of the surface that show islands on a surface which is observed to be largely unchanged from that of the clean 2D Ho silicide surface in figure 1(a). It is likely, and demonstrated in table 2, that the anneal will have accelerated the Ostwald ripening process and may have increased the surface diffusion of very small clusters of Mn. This allows areas of the 2D Ho silicide surface previously covered by Mn to become visible, yet there is little evidence of extensive damage to the 2D Ho silicide surface by the removal of surface Si atoms to form Mn silicide, a strong indication that the 2D Ho silicide layer has acted as an effective barrier. This is likely due to a number of related factors: (i) the much reduced depth of potential wells in the surface, i.e. (1 × 1) nature compared to the 7 × 7, means there is significantly less opportunity for Mn atoms to become trapped in these wells and react with Si to form Mn silicide; (ii) the subsurface RE layer provides an effective physical barrier for Mn diffusion into the subsurface silicon region again reducing the opportunity for Mn silicide formation, and, (iii) the passivated nature of the surface Si layer of the 2D silicide has appreciably reduced the reaction of deposited Mn atoms with the Si atoms in this topmost layer, even at step edges which are often an easy source of Si atoms. This evidence strongly suggests that the islands seen in figure 1(b) are likely to be composed of Mn rather than Mn silicide.

Figure 1(c) shows 2 ML of Mn deposited on to RT Si(111)-7 × 7 followed by an extensive anneal at 350 °C for 15 min. This surface showed a strong 1 × 1 LEED pattern with hints of $(\sqrt{3} \times \sqrt{3})$R30° fractional spots. A dark, lower level terrace can be seen in the Si surface where Si has been removed during silicide formation. This disorder to the Si surface has been seen in other Mn silicide studies where the Si surrounding islands has been removed to form the silicide [3, 7, 9].

A similar extensive anneal of 2 ML of Mn on Si(111)-1 × 1–Ho is shown in figure 1(d). This surface showed a 1 × 1 LEED pattern with poor contrast but without any evidence of

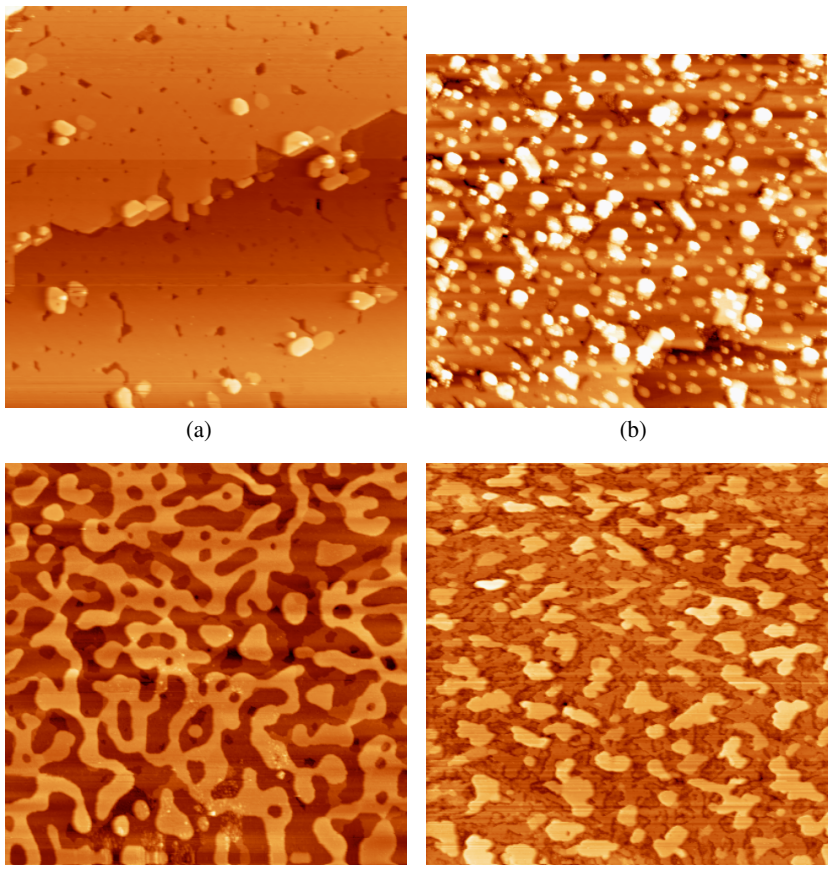

Figure 1. STM image of (a) the Si(111)-1 × 1–Ho surface, 300 nm × 300 nm, 2 V, 2 nA. (b) 2 ML of Mn deposited onto a RT Si(111)-1 × 1–Ho surface followed by a 1 min anneal at 300 °C, 300 nm × 280 nm, 1.7 V, 2 nA. (c) 2 ML of Mn deposited at RT on Si(111)-7 × 7 annealed at 350 °C for 15 min, 300 nm × 300 nm, 1.8 V, 1.5 nA. (d) 2 ML of Mn deposited onto RT Si(111)-1 × 1–Ho surface followed by a 15 min anneal at 350 °C, 300 nm × 300 nm, −1.8 V, 1.5 nA.

$(\sqrt{3}\times\sqrt{3})$R30° fractional spots. It is clear from figure 1(d) that there is a substantial increase in the defects in the Si(111)-1 × 1–Ho surface compared with the 1 min anneal. This increase is indicative of the removal of Si atoms from the surface bilayer of the 2D Ho silicide to form Mn silicide islands. However, the formation of Mn silicide is not as extensive as in the case of Mn on clean Si figure 1(c). Even for the simple MnSi phase, 2 ML of Si would be needed for complete silicide formation. Removal of 2 ML of silicon from the Si(111)-1 × 1–Ho surface would result in complete destruction of the surface Si bilayer. In addition, no $(\sqrt{3}\times\sqrt{3})$R30° fractional spots were observed in the 2D Ho silicide case, which further indicates that less Mn silicide formation has occurred.

3.2. The effect of cooling on the initial growth of Mn on the Si(111)-7 × 7 and Si(111)-1 × 1–Ho surfaces

3.2.1. Initial Mn growth on the Si(111)-7 × 7 surface. It is expected that the temperature of the substrate during deposition of Mn onto the Si(111)-7 × 7 surface will play an important role in the quality and morphology of the Mn growth. Figure 2 shows a comparison of Mn on Si(111)-7 × 7 deposited at RT and −180 °C, in both cases followed by a short, 1 min anneal. This short anneal was used to allow comparison with growth on the 2D Ho silicide surface where it is demonstrated that the short anneal is an important feature. For the cooled surface, the growth of Mn shows some differences to that on the RT surface. The reduced mobility of the Mn on the cooled surface during growth has clearly influenced the island formation after the short anneal. The island shapes are noticeably more irregular in shape and tend to be of greater height and smaller area compared to the RT growth. This results in a lower coverage of the surface area by islands for the cooled surface. This difference in morphology may be the result of the expected reduction in the initial formation of Mn silicide when Mn is deposited onto the cooled Si surface, and demonstrates that cooling during growth can influence the morphology of overlayer growth even after a short anneal to 350 °C.

3.2.2. Initial Mn growth on the Si(111)-1 × 1–Ho surface. Figure 3(a) shows an STM image of 2 ML of Mn deposited onto a RT Si(111)-1 × 1–Ho surface with no anneal. This surface shows a 1 × 1 LEED pattern. Mn islands can be seen above the Si(111)-1 × 1–Ho surface layer and appear as bright islands in this image. Large flat regions of the Si(111)-1 × 1–Ho surface can be seen with an irregular shaped defect towards the top left of the image. This defect is likely to be a result

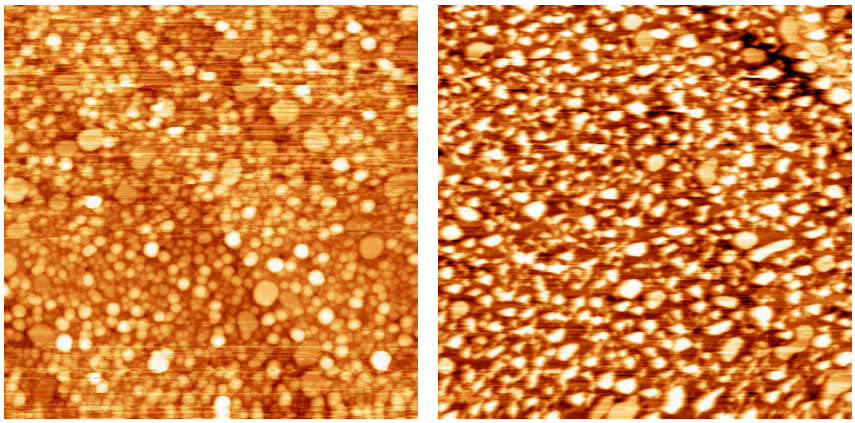

(a) (b)

Figure 2. STM images of 2 ML of Mn deposited on to a Si(111)-7 × 7 surface followed by a 1 min anneal at 350 °C. (a) Deposit at RT, 300 nm × 300 nm, 1.7 V, 2 nA (b) deposit at −180 °C, 300 nm × 300 nm, 1.7 V, 2 nA. Table 1 shows an island size and coverage analysis of these images.

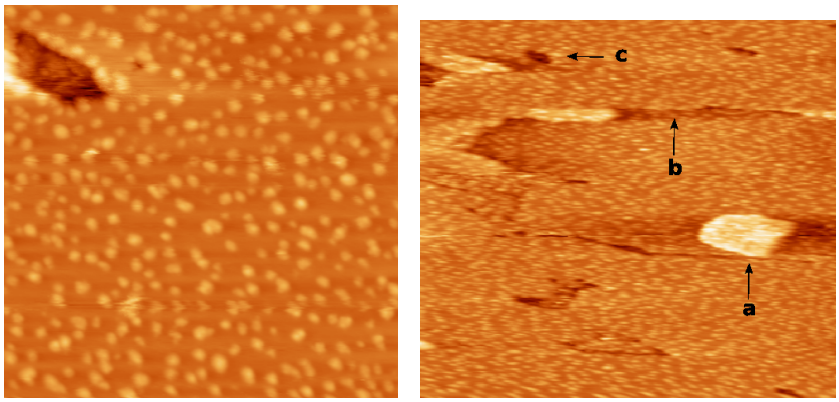

(a) (b)

Figure 3. STM images of 2 ML of Mn deposited on to a Si(111)-1 × 1–Ho surface at (a) RT, 50 nm × 50 nm, 1.8 V, 2 nA. (b) Cooled at −180 °C, 60 nm × 55 nm, 2 V, 2 nA. Due to scanning directly after cooling some drift can be seen in image (b). Table 2 shows an island size and coverage analysis of these images.

Table 1. Island characteristics for Mn deposited on to the RT (figure 2(a)) and cooled (figure 2(b)) Si(111)-7 × 7 surface followed by a 1 min anneal at 350 °C.

	Growth condition	
Island feature	RT + anneal	Cooled + anneal
Average area (nm^2)	28.19 ± 1.47	21.66 ± 2.61
Average height (nm)	0.74 ± 0.19	1.32 ± 0.21
Average diameter[a] (nm)	4.7 ± 1.3	4.6 ± 2.0
Surface coverage (%)	81.4 ± 2.4	50.5 ± 3.8

[a] Diameter measured as furthest two points on an island. Values calculated using the ImageJ software [25].

of strain relief caused by the lattice mismatch between Si(111) and the Si(111)-1 × 1–Ho surface. The Mn islands tend to form a uniform distribution over the surface with roughly equal sizes and with no apparent attraction to step edges or defects in the Si(111)-1 × 1–Ho layer. Neither is there a preference for where the Mn islands form although some ordering can be seen centrally towards the bottom of the image. All of the visible Si(111)-1 × 1–Ho surface appears still intact suggesting the Mn has not reacted with the silicon bilayer of the Si(111)-1 × 1–Ho surface. This is consistent with the passivation of the Si(111)-1 × 1–Ho surface by the subsurface Ho atoms as described earlier, leaving Mn atoms unable to react with the Si bilayer.

Figure 3(b) shows an STM image of 2 ML Mn deposited on the Si(111)-1 × 1–Ho surface cooled at −180 °C. This surface exhibited a weak 1 × 1 LEED pattern at low temperature. The flat Si(111)-1 × 1–Ho surface can again be seen with some defects visible. An island of 3D Ho silicide growth can be seen towards the right of the image (arrow a). A step edge is present near the top of the image (arrow b) and small dark irregular shaped defects (arrow c) can also be seen over the image. This 3D region (10 nm × 10 nm) is due to a slight over deposit of Ho during sample preparation and does not appear to affect the Mn island growth. Mn deposited on to a cooled Si(111)-1 × 1–Ho surface behaves differently compared to the RT Si(111)-1 × 1–Ho surface deposit. The cooled surface exhibits a higher number of islands which are significantly smaller in size. As with the RT surface, islands

Table 2. Island characteristics for 2 ML Mn deposited on to RT (figure 3(a)) and cooled (figure 3(b)) Si(111)-1 × 1–Ho surface before and after a 1 min anneal at 300 °C. Values were calculated using the ImageJ software. Note: the temperature and temperature + annealed values were not taken from the same samples so some variation in deposited coverages could be present.

	Growth condition			
Island feature	RT	RT + anneal	Cooled	Cooled + anneal
Average area (nm^2)	3.15 ± 0.09	26.55 ± 1.92	0.43 ± 0.01	42.8 ± 1.95
Average height (nm)	2.77 ± 0.08	0.78 ± 0.05	1.67 ± 0.05	0.61 ± 0.04
Average diameter (nm)	2.10 ± 0.05	4.9 ± 0.19	0.74 ± 0.02	7.6 ± 0.34
Surface coverage (%)	45.5 ± 2.4	32.2 ± 0.9	83.6 ± 6.7	68.1 ± 2.2

are generally uniform in dispersion and size with no obvious attraction to defects or features in the surface. The mobility of the Mn atoms on this surface is noticeably decreased by the cooling. This reduction of mobility suppresses Ostwald ripening during deposition leading to a large number of smaller Mn islands forming which results in a more complete coverage of Mn.

Mn deposited onto this surface and annealed at 300 °C for 1 min results in Mn islands sitting above a relatively unchanged Si(111)-1 × 1–Ho surface (figure 1(b)) and a slightly weaker 1 × 1 LEED pattern as previously discussed in section 3.1.

Table 2 shows the characteristics of Mn islands when grown on the RT and cooled Si(111)-1 × 1–Ho surfaces. With no subsequent anneal the islands on the RT Si(111)-1 × 1–Ho surface have larger surface areas and higher relative island heights when compared to the cooled surface. The reduced mobility is most apparent in the surface coverage percentage value. The RT surface, where atoms are free to form larger, higher islands, has only a 45.5% island coverage compared to 83.6% for the cooled surface. This result emphasizes the effect of cooling on Mn mobility during island growth.

In both the RT and cooled systems the 2D Ho silicide layer plays an important role in preventing Mn silicide formation by acting as a barrier between the Mn and the reactive bulk silicon. Although the Si(111)-1 × 1–Ho surface is terminated with a buckled silicon bilayer, similar in structure to bulk Si, it has a reduced reactivity due to passivation of the Si dangling bond by the Ho layer below.

3.2.3. Initial Mn growth on the Si(111)-1 × 1–Ho surface after annealing. Significant differences are seen when annealing 2 ML of Mn deposited on to the RT and cooled Si(111)-1 × 1–Ho surfaces. Figure 4(a) shows an STM image of 2 ML of Mn deposited on to a cooled Si(111)-1 × 1–Ho surface followed by an anneal at 300 °C for 1 min. Again, a short 1 min anneal is used to show the initial Mn growth before an equilibrium is reached. The island morphology of the cooled sample is noticeably different when compared to the RT sample (figure 1(b)). Mn islands have much larger areas and lower height, resulting in a higher surface coverage of Mn islands. On annealing, the mobility of small Mn islands on the cooled surface increases but they are surrounded by many more near-neighbour islands suppressing long range mobility. The Ostwald ripening effect leads to larger island formation resulting in a more complete layer of Mn. A full comparison of these island characteristics can be seen in table 2.

Marked differences in Mn island sizes are seen when comparing growth on the cooled Si(111)-7 × 7 and cooled Si(111)-1 × 1–Ho surfaces. As mentioned above, the Si(111)-7 × 7 surface contains potential wells in the faulted half of the unit cells of the Si(111)-7 × 7 surface resulting in Mn clusters formed in well-ordered arrays [8, 10]. The surface potential wells cause Mn atoms to have a higher relative mobility in the bulk compared to the surface encouraging Mn silicide formation [11]. Mn deposited on to a cooled Si(111)-7 × 7 surface has a reduced mobility suppressing Mn cluster formation in the potential wells and instead a uniform distribution of Mn is formed over the surface. When annealed, Mn silicide will form but with smaller more irregular islands. Mn mobility on the Si(111)-7 × 7 surface is dominated by the surface potential wells with the cooling only having a small effect. In contrast, the Si(111)-1 × 1–Ho surface does not contain any potential wells; Mn deposited on to this cooled surface will also produce a uniform distribution over the surface due to a reduced mobility. Here the cooling has a much greater effect and when annealed this uniform distribution will reduce the long distance mobility of the Mn causing interaction predominately with near-neighbour atoms. This results in large Mn island formation which potentially could form a complete layer for higher Mn coverages. By using cooling during Mn deposition on to the Si(111)-7 × 7 surface smaller silicide islands are produced following an anneal. In contrast, when cooling is used during deposition on to the Si(111)-1 × 1–Ho surface large Mn islands are formed after an anneal leading to the layer growth seen in figure 4(b).

3.2.4. The formation of the $(\sqrt{3} \times \sqrt{3})R30°$ reconstruction for 4 ML Mn coverage. Figures 4(b)–(d) show STM images of a higher 4 ML coverage of Mn deposited on to a cooled Si(111)-1 × 1–Ho surface followed by a 1 min anneal at 300 °C. Island sizes on the Si(111)-1 × 1–Ho surface are clearly much larger than the cooled 2 ML sample (figure 4(a)) with almost no Si(111)-1 × 1–Ho surface visible below the Mn island layers. As seen in the cooled 2 ML sample (figure 4(a)), Mn islands are not attracted to defects in the Si(111)-1 × 1–Ho surface, leading to additional Mn layers being constructed instead of a complete first layer. A defect free Si(111)-1 × 1–Ho surface could potentially lead to a complete, defect free Mn layer growth. Similarly to the 2 ML Mn surface, where the unchanged Si(111)-1 × 1–Ho surface could be seen in between the Mn islands, the Si(111)-1 × 1–Ho surface is thought to have remained intact below the 4 ML Mn layer. Once annealed this surface displayed a $(\sqrt{3} \times \sqrt{3})R30°$ LEED

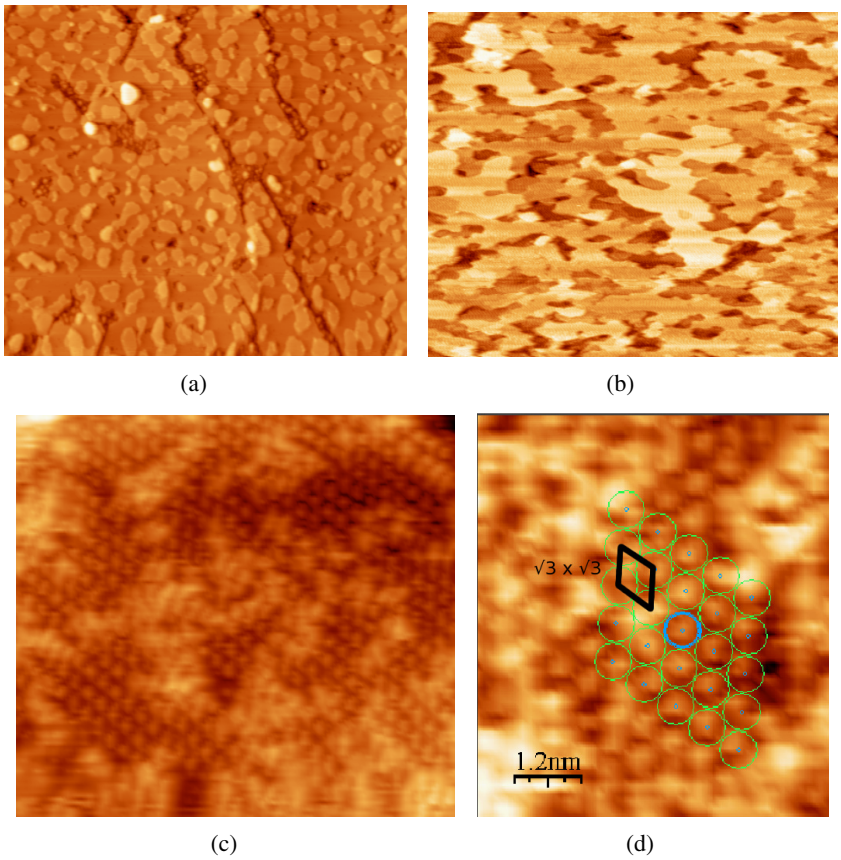

Figure 4. STM images of (a) 2 ML of Mn deposited on to the cooled Si(111)-1 × 1–Ho surface followed by a 1 min anneal at 300 °C, 300 nm × 280 nm, 1 V, 1 nA. (b)–(d) 4 ML of Mn deposited on to the cooled Si(111)-1 × 1–Ho surface followed by an 1 min anneal at 300 °C. (b) 200 nm × 196 nm 2 V, 1 nA. (c) 20 nm × 20 nm, −2 V, 3 nA. (d) 8 nm × 8 nm, −2 V, 3 nA.

Table 3. Summary of the crystal properties of the main bulk phases of Mn [29].

Phase	α	β	γ	δ
Formation temperature (°C)	below 800	800–1100	1100–1410	1410–1445
Related structure	bcc[a]	sc	fcc	bcc
Atoms per cell	58	20	4	2
Cell length (Å)	8.894	6.30	3.774	3.081
Av. atomic separation (Å)	2.24–3.00	2.36–2.67	2.67	2.67

[a] Structurally similar to bcc but with atomic position distorted to accommodate 4 extra Mn atoms.

pattern similar to the Mn layers grown on metal (111) surfaces and to Mn silicide. As with Mn on the RT surface, there is no evidence of a reaction between the surface Si bilayer and the Mn islands. Mn islands tend not to form around the Si-rich defects in the Si(111)-1 × 1–Ho surface once annealed. Again, this leads us to believe islands consist of only Mn with no, or little, Si involved. Cooling the Si(111)-1 × 1–Ho surface during Mn deposition suppresses the effect of Ostwald ripening, increasing the formation of small Mn islands. This stage has proved vital in the production of what we believe to be epitaxial Mn layer growth.

3.2.5. Mn layer structure. Figures 4(c) and (d) show high magnification images of the Mn island surface shown in figure 4(b). A clear 2D hexagonal unit cell structure can be seen in the Mn layer surface. Of all the elements, Mn displays the most complex bulk structures. Table 3 summarizes the crystal properties of the four main Mn bulk phases. The lower temperature alpha phase contains 58 atoms/unit cube. Despite this complexity the structure is similar to bcc with atomic positions altered for the addition of 4 extra Mn atoms. The second low temperature growth phase, β, contains 20 atoms and is paramagnetic. The high complexity of the α and β bulk phases of Mn create difficulties when fitting to the Si(111)-1 × 1 surface. At higher temperatures, the unit cells of bulk Mn are smaller, with a phase transition to fcc at 1100 °C and then bcc at 1410 °C. Although these phases are present at high temperatures in bulk Mn, previous studies have suggested it is possible to grow these simpler phases in thin films [26]. Mn phases which are not present in the bulk have also been seen,

such as the expanded hexagonal phase for low coverages and metastable Mn films grown on GaAs(001) where fcc films were produced with lattice parameters of 0.362 nm [27, 28]. None of the hexagonal planes of the main bulk Mn phases have an acceptable lattice match to the $\sqrt{3}$ distance of the Si(111)-1 × 1–Ho surface, 6.65 Å. The visible hexagonal termination also offers the possibility of a hexagonal or hexagonal close packed structure (hcp) with nearest-neighbour distance comparable to those in table 3.

4. Summary

The growth of an ordered Mn layer on a cooled Si(111)-1 × 1–Ho surface has been studied using STM. The key finding has shown it is possible to suppress Mn silicide formation during both Mn deposition and annealing, resulting in the formation of an ordered Mn layer. The suppression of the formation of Mn silicide was achieved by two methods. Firstly, a 2D Ho silicide layer was used as a buffer layer to suppress interaction between the Mn and the Si(111) substrate. Secondly, the Si(111)-1 × 1–Ho surface was cooled using liquid nitrogen −180 °C which reduces the initial Mn–Si reaction and reduces the mobility of the Mn atoms. Reducing the mobility of the deposited Mn atoms reduces large island formation instead forming a near uniform distribution of Mn over the surface. After a short 1 min anneal at 300 °C an ordered $(\sqrt{3} \times \sqrt{3})$R30° LEED pattern is observed with STM images displaying a layered growth with a hexagonal structure in the case of the 4 ML deposit. Further work is currently being carried out to determine the structure of the ordered Mn layer on the Si(111)-1 × 1–Ho surface. The cooling has been seen to be much more effective at reducing the mobility on the Si(111)-1 × 1–Ho surface compared to the Si(111)-7 × 7 surface, due to the absence on the potential wells on the Si(111)-1 × 1–Ho surface. This has led to significant differences in the growth of Mn islands on the Si(111)-1 × 1–Ho and Si(111)-7 × 7 surfaces when deposited at RT and cooled conditions. The cooled Si(111)-1 × 1–Ho surface has been seen to be a good surface for the growth of ordered Mn layers on a Si surface. This system could potentially lead to the growth of ordered magnetic metal layers on Si, particularly interesting for the development of spintronic devices.

Acknowledgment

The authors would like to acknowledge the Engineering and Physical Science Research Council for funding this research.

References

[1] Blügel S 1992 *Phys. Rev. Lett.* **68** 851–4
[2] Wuttig M, Gauthier Y and Blügel S 1993 *Phys. Rev. Lett.* **70** 3619–22
[3] Kumar A, Tallarida M, Hansmann M, Starke U and Horn K 2004 *J. Phys. D: Appl. Phys.* **37** 1083–90
[4] Prokes S M, Glembocki O J, Carlos W E and Kennedy T A 2003 *Appl. Surf. Sci.* **214** 103
[5] Wu H, Hortamani M, Kratzer P and Scheffler M 2004 *Phys. Rev. Lett.* **92** 237202
[6] Schwinge K, Paggel J J and Fumagalli P 2007 *Surf. Sci.* **601** 810
[7] Evans M M R, Glueckstein J C and Nogami J 1996 *Phys. Rev.* B **53** 4000–4
[8] Nagao T, Ohuchi S, Matsuoka Y and Hasegawa S 1999 *Surf. Sci.* **419** 134–43
[9] Zou Z-Q, Wang H, Wang D, Wang Q-K, Mao J-J and Kong X-Y 2007 *Appl. Phys. Lett.* **90** 133111
[10] Wang H and Zou Z-Q 2006 *Appl. Phys. Lett.* **88** 103115
[11] Azatyan S, Hirai M, Kusaka M and Iwami M 2004 *Appl. Surf. Sci.* **237** 105–9
[12] Azatyan S, Iwami M and Lifshits V G 2005 *Surf. Sci.* **589** 106–13
[13] Fonin M, Dedkov Yu S, Rudiger U and Guntherodt G 2003 *Surf. Sci.* **529** L275–80
[14] Biswas C, Dhaka R S, Shukla A K and Barman S R 2007 *Surf. Sci.* **601** 609–14
[15] Schneider J, Rosenhahn A and Wandelt K 1999 *Appl. Surf. Sci.* **142** 68–74
[16] Norde H, de Sousa Pires J, d'Heule F M, Pesavento F, Petersson S and Tove P A 1981 *Appl. Phys. Lett.* **38** 865
[17] Tu K N, Thompson R D and Tsaur B Y 1981 *Appl. Phys. Lett.* **38** 626
[18] Knapp J 1986 *Phys. Rev. Lett.* **48** 237202
[19] Bonet C, Scott I M, Spence D J, Wood T J, Noakes T C Q, Bailey P and Tear S P 2005 *Phys. Rev.* B **72** 165407
[20] Spence D J, Tear S P, Noakes T C Q and Bailey P 2000 *Phys. Rev.* B **61** 5707–13
[21] Wood T J, Bonet C, Noakes T C Q, Bailey P and Tear S P 2006 *Phys. Rev.* B **73** 235405
[22] Perkins E W, Bonet C and Tear S P 2005 *Phys. Rev.* B **72** 195406
[23] Zavaliche F, Wulfhekel W, Xu H and Kirschner J 2000 *J. Appl. Phys.* **88** 5289–92
[24] Yang J J, Rawn C J, Ji C-X, Chang Y A, Chen Y, Ragan R, Ohlberg D A A and Williams R S 2006 *Appl. Phys.* A **82** 39–42
[25] ImageJ software available from http://rsbweb.nih.gov/ij/
[26] Grigorov I L, Fitzsimmons M R, Siu I-L and Walker J C 1996 *Phys. Rev. Lett.* **82** 5309
[27] Arrott A S, Heinrich B, Purcell S T, Cochran J F and Urquhart K B 1987 *J. Appl. Phys.* **61** 3721
[28] Jin X, Zhang M, Dong G S, Xu M, Chen Y, Wang X, Zhu X G and Shen X L 1994 *Appl. Phys. Lett.* **65** 3078–80
[29] Wyckoff R W G 1963 *Crystal Structures* (New York: Interscience)